# Grafting Kinetics of Vinyl Neodecanoate onto Polybutadiene

**Binh T. T. Pham, Matthew P. Tonge, Michael J. Monteiro,† and Robert G. Gilbert***

*Key Centre for Polymer Colloids, School of Chemistry, University of Sydney, NSW 2006, Australia*

*Received April 20, 1999; Revised Manuscript Received January 12, 2000*

ABSTRACT: The kinetics and mechanism of the bulk free-radical polymerization of vinyl neodecanoate in the presence of polybutadiene are studied in a series of rate and molecular weight distribution measurements over the temperature range 50−90 °C. The polymerization of the vinyl ester is greatly retarded by the presence of polybutadiene. The dependences of the rates and molecular weight distributions on the ratio of monomer to the amount of polybutadiene are quantitatively in accord with a retardative chain transfer mechanism, whereby an alkanoate radical undergoes hydrogen transfer with polybutadiene, leaving an unreactive radical species (probably allylic in character) which cannot propagate and instead undergoes termination with another radical. The data yield Arrhenius parameters for the transfer to polybutadiene as $k_{tr,P} = 10^{6.9}$ dm$^3$ mol$^{-1}$ s$^{-1}$ exp(−27.6 kJ mol$^{-1}$), which, although subject to high uncertainty, are consistent with the rate-determining step being either (a) diffusion to a hindered butadiene unit of the chain end of an alkanoate macroradical or (b) the actual (chemically controlled) hydrogen transfer event, which would then have to have an unusually low activation energy.

## Introduction

Chain transfer to polymer leads to branching and/or cross-linking in the final polymer, the extent of which can affect end-use properties. There are few reliable data in the literature for the rate coefficient of transfer to polymer and the site of transfer, a consequence of the difficulties involved experimentally. Recently, Lovell et al. gave evidence that chain transfer to polymer in free-radical homopolymerizations and copolymerization of *n*-butyl acrylate involves abstraction of hydrogen atoms from backbone tertiary C−H bonds,[1−4] while chain transfer to polymer in the free-radical homopolymerization of vinyl acetate takes place via hydrogen abstraction from the methyl side group.[5]

Such chain transfer is expected to be especially strong in vinyl alkanoates such as vinyl acetate and vinyl neodecanoate (VnD):

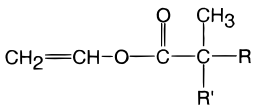


(the commercial VnD monomer is a mixture of isomers, where the total number of carbons in R and R′ is 7). The Arrhenius parameters for propagation of VnD and vinyl acetate are very similar.[6] Recent work in this laboratory with solution and emulsion polymerization of VnD in the presence of polyisoprene[7,8] showed a large amount of retardation and evidence of extensive grafting. The data were qualitatively consistent with a mechanism of retardative chain transfer, in which growing polyVnD radicals are grafted onto the backbone of polyisoprene and thereafter have greatly diminished propagation rates.

It is well established that oxyl radicals readily promote grafting of many polymers onto the backbone of polybutadiene. The most studied system is styrene/benzoyl peroxide/*cis*-polybutadiene, in which grafting is initiated exclusively by primary radicals derived from benzoyl peroxide. On the other hand, AIBN does not promote grafting of many monomers on to *cis*-polybutadiene.[9,10] Bevington[11] reported that AIBN-derived radicals were unreactive toward abstracting methyl hydrogen atoms. This was explained to be due to the resonance stability of the cyano-derived radical. The effect of grafting reactions of styrene, benzyl methacrylate and benzyl acrylate onto the backbone of polybutadiene initiated with AIBN has been extensively studied by Huang and Sundberg.[12−15] These authors considered graft site initiation, grafting across the double bond, and abstraction of the allylic hydrogen from polybutadiene. It was found that the levels of grafting were in the order benzyl acrylate > benzyl methacrylate > styrene, which is the reverse order of the polymeric radical stability. Huang and Sundberg[12−15] proposed that the high reactivity of the acrylate is due to both abstraction from the allylic hydrogen and addition across the double bonds in polybutadiene. On the basis of this grafting mechanism, the resultant copolymer would consist of a low number of grafted chains, which have long chain lengths.

The purpose of this paper is a kinetic study of the mechanism of grafting reactions in the polymerization of vinyl neodecanoate in the presence of polybutadiene. The study attempts to determine (a) whether retardative chain transfer is a mechanism at play for the VnD/polybutadiene system and (b) the rate coefficient for transfer of a hydrogen atom from the polybutadiene backbone by VnD radicals. The bulk polymerization of VnD is carried out in the presence of various amounts of low molecular weight polybutadiene, using AIBN as initiator; low molecular weights of polybutadiene are necessary because higher molecular weight samples are found to be insoluble in VnD monomer.

The Arrhenius parameters will then be examined in an attempt to determine the mechanism of the reaction process, which is between two polymer chains (a VnD macroradical and polybutadiene): specifically, to see if it is controlled by the diffusion of the radical chain end or by the "chemical" step of the actual abstraction.

* Author for correspondence and proofs
† Present address: Eindhoven University of Technology, Dept of Polymer Chemistry and Coating Technology, PO Box 513, 5600 MB Eindhoven, The Netherlands.

10.1021/ma990604r CCC: $19.00 
Published on Web 03/04/2000

## Experimental Section

**Materials.** Low molecular weight polybutadiene (Aldrich, $\bar{M}_n = 5 \times 10^3$) was used as received. Vinyl neodecanoate (Aldrich), actually a mixture of isomers, was purified by passing it through a fresh column of basic alumina. Azobis(isobutyronitrile) (AIBN) was recrystallized twice from ethanol/water at ambient temperature. Deuterated chloroform (Aldrich), tetrahydrofuran (THF) (Ajax Laboratory Chemicals), and polystyrene molecular weight standards (Waters) were used as received.

The $^1$H NMR spectrum of low molecular weight polybutadiene was recorded at 80 °C on a Bruker 200 MHz spectrometer in deuterated chloroform. The general features of the spectrum of polybutadiene have been previously defined.[16] The NMR data of the present sample showed that the polybutadiene contained all the three structural units 1,2 vinyl (20%) and *cis*- and *trans*-1,4 (a total of 80%):

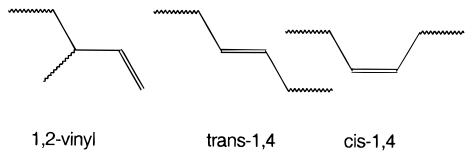


**Polymerization of VnD in Polybutadiene.** Bulk polymerizations of VnD in the presence of polybutadiene were carried out at 50, 70, and 90 °C. In a typical recipe, VnD and polybutadiene were placed in a round-bottom flask and allowed to stir under a nitrogen atmosphere for at least 2 h until a homogeneous mixture was obtained. The mixture was transferred to a dilatometric vessel containing AIBN and then brought up to the required temperature. No specific measures were taken to ensure that all oxygen had been removed from the reaction solution. A capillary was then installed and filled with decane to obtain a fine meniscus. The conversion of monomer to polymer was determined dilatometrically, assuming ideal mixing, using the density of monomer at each temperature as determined elsewhere.[6] The conversions of a number of samples were also measured by gravimetry, and acceptable accord between gravimetric and dilatometric conversions was always obtained. All polymerizations were carried out to conversions below 20% to avoid inefficient mixing due to the formation of a gel.

The formulations and some conversion data for the various runs are shown in Table 1. The system is always above the glass transition (i.e., always rubbery) at all temperatures and conversions studied here.

**Molecular Weight Distributions.** Average molecular weights of samples after polymerizing were determined using a Waters GPC with differential refractometer R401, a 510 HPLC pump, and an Ultrastyragel linear-mixed-bed column. Analysis of samples was carried out at room temperature. Monodisperse polystyrene standards from Waters with known peak molecular weights ($3 \times 10^3$ to $10^6$) were used to calibrate the instrument. Absolute molecular weights of the polymer were obtained from the molecular weights relative to polystyrene using the Mark−Houwink−Sakaruda parameters $K = 1.1 \times 10^{-5}$ dL g$^{-1}$ and $\alpha = 0.725$ for polystyrene[17] and $K = 7.26 \times 10^{-5}$ dL g$^{-1}$ and $\alpha = 0.716$ for polyVnD.[6] The results for the molecular weight distribution so obtained, which assumes an unbranched chain of pure VnD, are only semiquantitative, since the actual polymer may be a polybutadiene/VnD graft copolymer.

## Results and Discussion

The data for a range of monomer, polybutadiene, and initiator concentrations at 50−90 °C in Table 1 and in Figures 1−4 show that the polymerization rate is decreased when small amounts of polybutadiene are present. This is qualitatively consistent with the retardative chain transfer mechanism suggested for polyisoprene.

**Table 1. Effect of Polybutadiene on the Conversion of VneoD Initiated with AIBN[a]**

50 °C

| run | [AIBN] (mM) | [VnD] (M) | [B] (M) | [VD]/[B] | % conv after 22 h |
|---|---|---|---|---|---|
| bulk | 11 | 4.45 | 0 | | |
| 1 | 6.2 | 4.01 | 1.61 | 2.49 | 1.3 |
| 2 | 8.6 | 4.35 | 0.37 | 11.7 | 4.0 |
| 3 | 10.9 | 4.42 | 0.10 | 44.6 | 15.8 |
| 4 | 10.9 | 4.39 | 0.21 | 21.4 | 10.2 |
| 5 | 11.0 | 4.35 | 0.35 | 12.6 | 6.9 |

70 °C

| run | [AIBN] (mM) | [VnD] (M) | [B] (M) | [VD]/[B] | % conv after 2.2 h |
|---|---|---|---|---|---|
| 7 | 11.6 | 4.36 | 0.34 | 13.0 | 9.7 |
| 8 | 11.5 | 4.23 | 0.80 | 5.26 | 4.4 |
| 9 | 11.6 | 4.04 | 1.50 | 2.7 | 2.7 |

90 °C

| run | [AIBN] (mM) | [VnD] (M) | [B] (M) | [VD]/[B] | % conv after 20 min |
|---|---|---|---|---|---|
| 10 | 11.6 | 4.20 | 0.93 | 4.51 | 8.5 |
| 11 | 11.6 | 3.97 | 1.77 | 2.24 | 4.6 |
| 12 | 11.6 | 3.59 | 3.16 | 1.14 | 2.2 |

[a] [B] = concentration of polymer in terms of moles of butadiene monomer units.

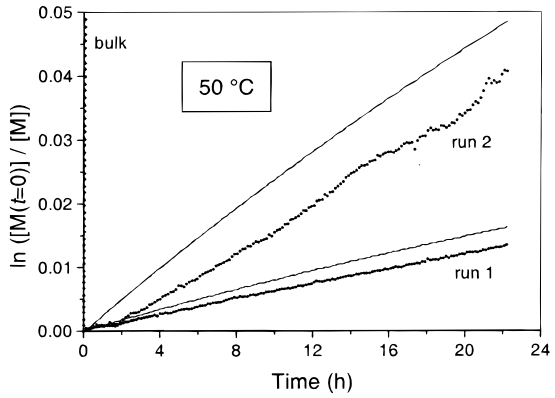


**Figure 1.** Conversion vs time for polymerization of vinyl neodecanoate (VnD) with and without (bulk) polybutadiene (PB) at 50 °C. Run 1: [B]/[VnD] = 0.4. Run 2: [B]/[VnD] = 0.09. Points: experiment. Lines: simulation.

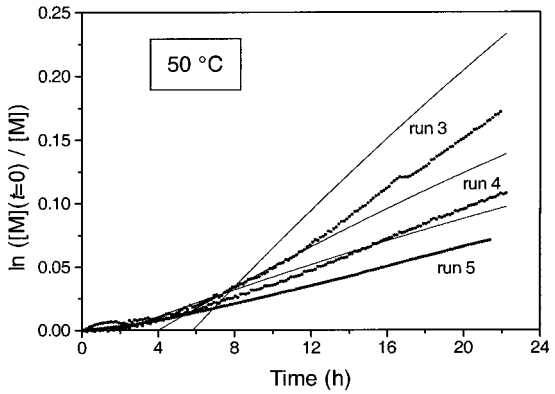


**Figure 2.** Rate, as ln{[$M(t = 0)$]/[M]} vs time $t$, for polymerization of VnD in the presence of PB at 50 °C for run numbers as indicated. Points: experiment. Lines: simulation.

To further characterize this as the mechanism at play, the data were compared with the behavior predicted from the kinetic scheme for retardative chain transfer. It is also important to note that all data exhibit an

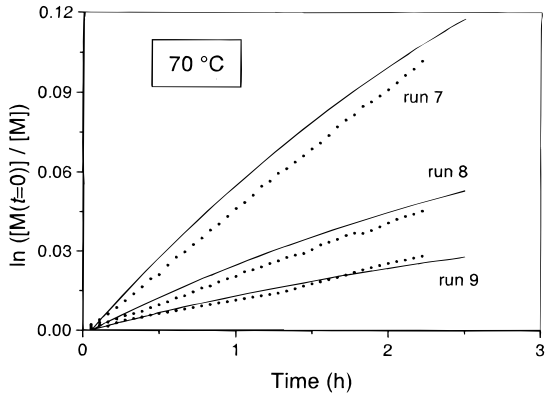


**Figure 3.** Rate, as ln{[$M(t = 0)$]/[M]} vs time $t$, for polymerization of VnD in the presence of polybutadiene at 70 °C (run numbers 7−9 as indicated). Points: experiment. Lines: simulation.

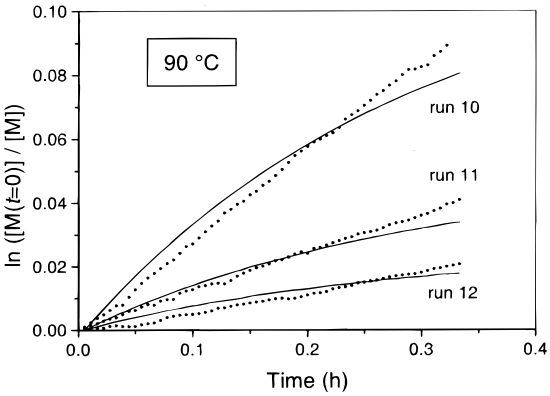


**Figure 4.** Rate, as ln{[$M(t = 0)$]/[M]} vs time $t$, for polymerization of VnD in the presence of polybutadiene at 90 °C (run numbers 10−12 as indicated). Points: experiment. Lines: simulation.

inhibition period, probably due to the presence of dissolved oxygen (which was not specifically eliminated prior to reaction). This period was ignored in simulations and kinetic parameter determination.

**Kinetic Analysis.** The retardative chain transfer mechanism postulated here is as follows:

$$\mathrm{I} \xrightarrow{fk_\mathrm{d}} 2\mathrm{R}^\bullet \tag{1}$$

$$\mathrm{M}_n^\bullet + \mathrm{M} \xrightarrow{k_\mathrm{p}} \mathrm{M}_{n+1}^\bullet \tag{2}$$

$$\mathrm{M}_n^\bullet + \mathrm{B} \xrightarrow{k_{\mathrm{tr,P}}} \mathrm{B}^\bullet + \mathrm{M}_n\mathrm{H} \tag{3}$$

$$\mathrm{B}^\bullet + \mathrm{M} \xrightarrow{k_\mathrm{a}} \mathrm{BM}^\bullet \tag{4}$$

$$\mathrm{M}_n^\bullet + \mathrm{B}^\bullet \xrightarrow{k_{\mathrm{tP}}} \mathrm{BM} \tag{5}$$

$$\mathrm{M}_n^\bullet + \mathrm{M}_m^\bullet \xrightarrow{k_\mathrm{t}} \mathrm{M}_{n+m} \tag{6}$$

where I = initiator, M = VnD, B = butadiene monomer unit in polybutadiene, and R$^\bullet$ = initiator-derived radical.

The rate equations corresponding to these reactions are solved numerically, as discussed later. Kinetic analysis is facilitated through approximate analytic solutions obtained by assuming a time-independent [I] (eq 1—this introduces only small errors, since the amount of initiator decomposition on the reaction time scales is significant, but not large), negligible reinitiation ($k_\mathrm{a} = 0$, which was found to be a good approximation for most reaction conditions) and ignoring the homotermination reaction ($k_\mathrm{t} = 0$, which was found by simulations to be an excellent approximation under all reaction conditions in this study). One then obtains

$$\ln \frac{[M(t=0)]}{[\mathrm{M}]} = \frac{fk_\mathrm{d}k_\mathrm{p}[\mathrm{I}]}{k_{\mathrm{tr,P}}[\mathrm{B}]} \quad t \equiv St \tag{7}$$

where $S$ is the slope of a plot of ln[$M(t = 0)$]/[M] vs time and is equal to $fk_\mathrm{d}k_\mathrm{p}$ [I]/$k_{\mathrm{tr,P}}$[B].

Under these assumptions, a plot of ln[$M(t = 0)$]/[M] vs time should be linear. Indeed linearity is seen experimentally to be an acceptable approximation, as shown in Figures 1−4, making due allowance for the existence of a variable induction period. The experimental slope $S_\mathrm{exp}$ of such a plot (i.e., of the linear region of ln[$M(t = 0)$]/[M]) should yield $fk_\mathrm{d}k_\mathrm{p}/k_{\mathrm{tr,P}}$ (assuming that [I] and [B] are constant, which is normally a good assumption, as long as an appropriate value of [I] is used in this region, accounting for initiator decomposition). Hence plots of $S_\mathrm{exp}$ against [I]/[B] for a series of runs with different [I] and [B] should also be linear. Again this is in acceptable accord with experiment, as seen in Figure 5. The final values of $k_{\mathrm{tr,P}}$ were calculated from the slopes of the plots in Figure 5.

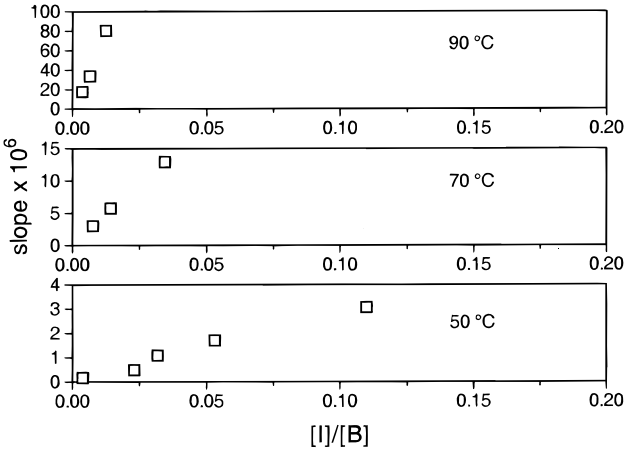


**Figure 5.** Dependence of slopes of plots ln([$M(t = 0)$]/[M]) vs time on the ratio of initiator concentration [I] to concentration of butadiene monomer unit [B]. From data of Figures 1−4.

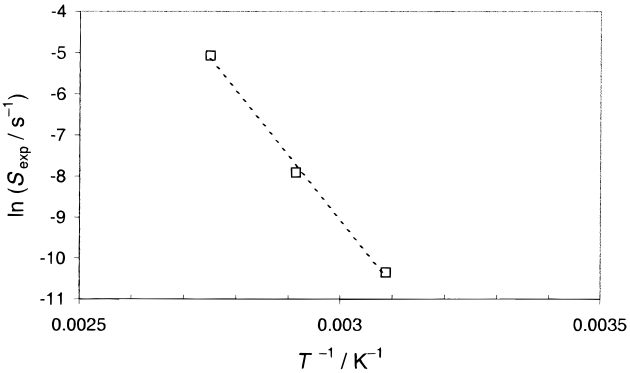


**Figure 6.** Arrhenius plot of experimental slopes from Figure 5.

The values obtained for $S_\mathrm{exp}$ for each temperature are shown in an Arrhenius form in Figure 6; the data fit $S_\mathrm{exp}/\mathrm{s}^{-1} = 10^{16.2}\exp(-129\ \mathrm{kJ\ mol}^{-1}/RT)$. These values of $S_\mathrm{exp}$ can be used to obtain values of $k_{\mathrm{tr,P}}$ at each temperature, given values of $f$, $k_\mathrm{d}$, and $k_\mathrm{p}$. Assuming

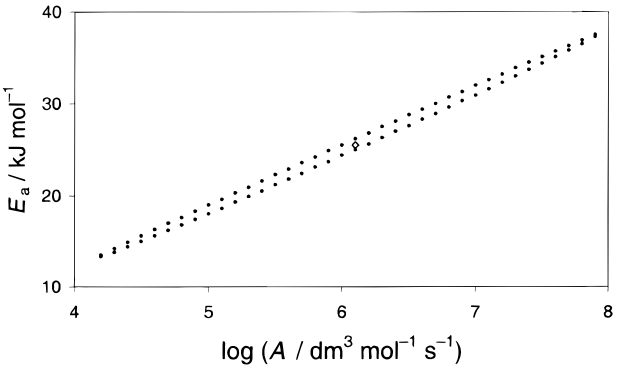


**Figure 7.** 95% contour and minimum ($A$) for $\chi^2$ for the joint confidence interval for the activation energy and frequency factor obtained by nonlinear fit of the Arrhenius equation to the values of $k_{tr,P}$ as described in the text.

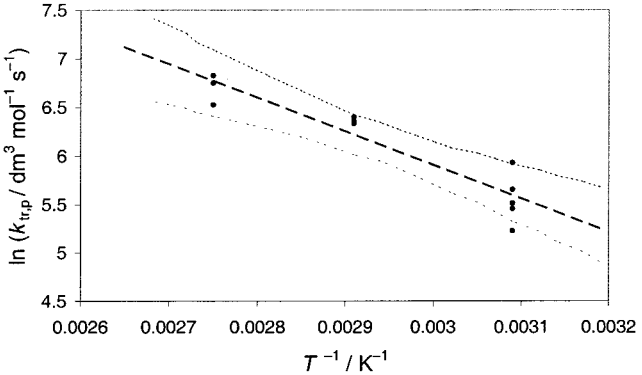


**Figure 8.** Arrhenius plot of the calculated $k_{tr,P}$ values. The best fit to the Arrhenius equation is shown as the dashed line, and the contours defined by the 95% confidence limits are shown as dotted lines. The points are experimental values for each temperature.

$f = 0.7$,[18] $k_d$/s$^{-1} = 4.31 \times 10^{15}$ exp(−131.7 kJ mol$^{-1}$/$RT$),[18] and $k_p$ / dm$^3$ mol$^{-1}$ s$^{-1}$ = $10^{7.31}$ exp(−22.2 kJ mol$^{-1}$/$RT$),[6] one obtains $k_{tr,P}$/dm$^3$ mol$^{-1}$ s$^{-1}$ = 259, 614, and 723 at 50, 70 and 90 °C, respectively.

Unfortunately, this last data reduction (to obtain $k_{tr,P}$) is subject to high uncertainty, since the values of $k_{tr,P}$ so obtained are very sensitive to (a) uncertainties in the activation energies of $k_d$ and $k_p$, especially because of the high activation energy for $k_d$, and (b) the relatively large experimental uncertainties in the values of $S_{exp}$. Because of this high uncertainty, an error analysis of the resulting values of $k_{tr,P}$ is essential. This was done in the following, admittedly simplistic way. (1) Uncertainties of ±2 and ±1 kJ mol$^{-1}$ were assumed in the activation energies for $k_d$ and $k_p$ respectively. (2) These uncertainties, together with those in the values of $S_{exp}$, were used to find the maximum and minimum possible values of $k_{tr,P}$. (3) These maximum and minimum values, together with the mean values, were used to generate $\chi$, the least-squares residual of ln($k_{calculated}$/$k_{observed}$) defined by

$$\chi^2 = \sum\left(\ln\frac{k_{calculated}}{k_{observed}}\right)^2 \qquad (8)$$

(the summation being over all experimental points). (4) Minimization of $\chi^2$ in eq 8 is carried out with respect to the Arrhenius activation energy and frequency factor for $k_{tr,P}$; this gives a nonlinear fit of the Arrhenius equation to these collected values of $k_{tr,P}$. The minimum in $\chi^2$ so obtained gives $k_{tr,P}$/dm$^3$ mol$^{-1}$ s$^{-1}$ = $10^{6.9}$ exp(−27.6 kJ mol$^{-1}$/$RT$), with the 95% contour for $\chi^2$ shown in Figure 7.

It is important to be aware that values for the activation energy and frequency factor deduced from experimental rate data are highly correlated. Thus, it is generally incorrect to quote independent uncertainties for each of these quantities, and instead the correlated uncertainties are quantitatively expressed in a joint confidence interval as shown in Figure 7.[19] An Arrhenius plot of the experimental $k_{tr,P}$ values, with the best fit line and 95% confidence limits, is shown in Figure 8.

**Numerical Simulations.** As a partial check on the various approximations leading to eq 7, a full numerical solution of the kinetic equations for reactions 1−6 was carried out; note that because of the long polymerization time (comparable to the initiator half-life), the inclusion of reaction 1 is needed in this procedure. The values used in these simulations have been given above, together with the $k_{tr,P}$ values obtained from the data fitting as described above. The value of $k_a$ was taken as zero (as set out in detail later, there was no significant effect on the predicted rate results if $k_a$ values of up to ca. $10^{-5}$ dm$^3$ mol$^{-1}$ s$^{-1}$ were included in the simulations). The value of $k_t$ was the average over all radical chain lengths, $\langle k_t \rangle$, predicted from the diffusion-controlled model of Russell et al.[20−23] with the values of the dependence of the diffusion coefficients of oligomers as a function of polymer weight fraction $w_p$ taken to be the given by the "universal" scaling expression given by Griffiths et al.[24] for a variety of rubbery systems. Again, calculated rates for VnD polymerization in the presence of significant amounts of polybutadiene were quite insensitive to the values of $\langle k_t \rangle$.

As a test of the sensitivity of the kinetic model to variations in the input parameters, simulations were generated with variations in the input parameters for all of the experiments, and for several of the experiments (at least one at each temperature), more extensive sensitivity analyses were performed. The parameters that were varied in the sensitivity analyses were the values of $k_t$, $k_a$, $k_{tr,P}$, $k_d$, and $k_{tP}$. The input parameters for the simulations shown in Figures 1−4 were as given above.

The comparison between the experimental data and the simulations are shown in Figures 1−4. Note that some runs (especially those shown in Figure 2) show an extensive induction period with a small retardation period at the start of the polymerization; this effect is not included in the kinetic scheme and therefore not reproduced by the simulations. In most cases, the agreement between simulation and experiment is fairly good. Although quantitative accord is not achieved, the general features of the curves are reproduced, and the quantitative discrepancies are not large when compared with the errors introduced through the uncertainties in the input parameters, which will be illustrated below.

The sensitivity of the simulated curves to variations in $k_t$ and $k_{tP}$ were relatively small, as shown in Figure 9. At all temperatures, it was found that the approximation $k_t = 0$ was excellent: curves generated with unmodified input parameters and those using $k_t = 0$, are indistinguishable. This also implies that chain-length dependence of termination will not be a significant factor, since other kinetic events are always overwhelmingly dominant. Changes in $k_{tP}$ by an order

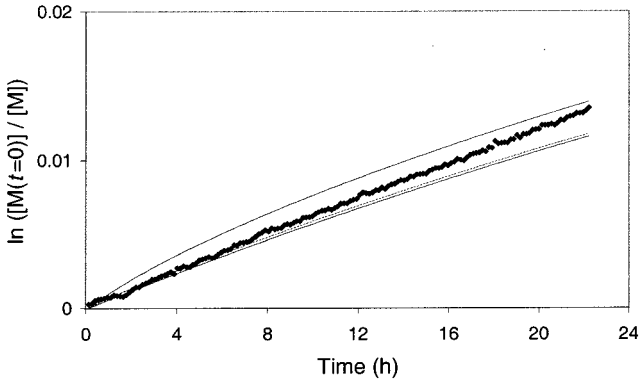


**Figure 9.** Sensitivity of simulated rate curves to variations in the input parameters $k_t$ and $k_{tP}$ for run 1 (50 °C): comparison of unmodified simulation curve (dotted line) with experiment (points) and curves generated using $k_{tP} = 10^6$ dm$^3$ mol$^{-1}$ s$^{-1}$ (unbroken line) and $k_{tP} = 10^8$ dm$^3$ mol$^{-1}$ s$^{-1}$ (dashed line).

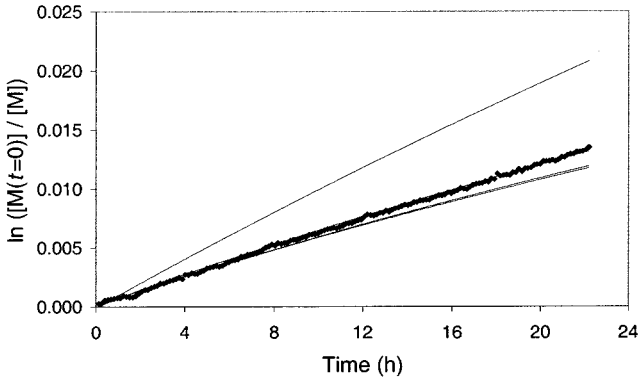


**Figure 10.** Sensitivity of simulated rate curves to variations in the input parameter $k_a$ for run 1 (50 °C): from top to bottom, $k_a = 10^{-4}$, $10^{-5}$, and $10^{-6}$ dm$^3$ and 0 mol$^{-1}$ s$^{-1}$. The experimental data are shown for comparison. Note: the value for $k_{tr,P}$ used here is the best-fit value to the entire data set, rather than the individual $k_{tr,P}$ for run 1.

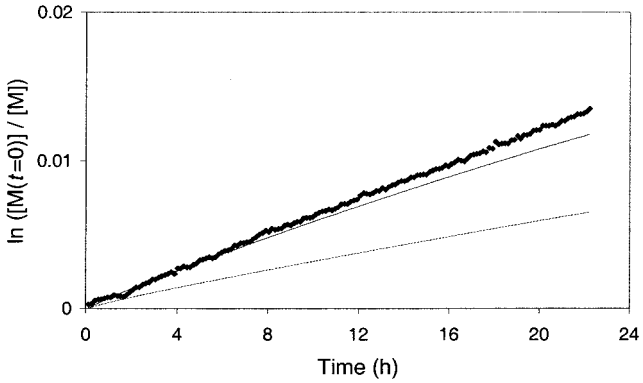


**Figure 11.** Sensitivity of simulated rate curves to variations in the input parameter $k_d$ for run 1 (50 °C): with the literature value of $k_d$ (unbroken line) and with $k_d$ reduced to half of this value (dotted line). The experimental data are shown for comparison. Note: the value for $k_{tr,P}$ used here is the best-fit value to the entire data set, rather than the individual $k_{tr,P}$ for run 1.

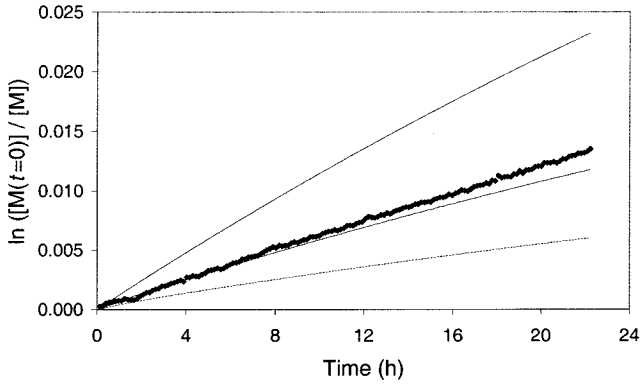


**Figure 12.** Sensitivity of simulated rate curves to variations in the input parameter $k_{tr,P}$ for run 1 (50 °C): with best-fit value as described in the text (unbroken line), half this value (dashed line), and twice this value (dotted line). The experimental data are shown for comparison. Note: the value for $k_{tr,P}$ used here is the best-fit value to the entire data set, rather than the individual $k_{tr,P}$ for run 1.

of magnitude in either direction changed the rate of reaction slightly, but by far less than changes in other input parameters.

The sensitivity of the simulated curves to the other input parameters was greater. The sensitivity to the value of $k_a$ is shown in Figure 10. Obviously, lower values of $k_a$ generate a lower overall rate of reaction. It was found that the approximation $k_a = 0$ was reasonable under most circumstances, with little effect on the kinetics until $k_a$ was increased to ca. $10^{-5}$ dm$^3$ mol$^{-1}$ s$^{-1}$ ($10^{-4}$ dm$^3$ mol$^{-1}$ s$^{-1}$ at 90 °C). Beyond this region, the calculated rate of reaction increases drastically, due to significant reinitiation and subsequent propagation of the grafted side chains. Now, the simulated curves shown in Figures 1−4 were generated using the approximation $k_a = 0$ and almost always lie above the experimental curves, especially at 50 °C. This, in the absence of other uncertainties, would suggest that the lower values of $k_a$ (less than ca. $10^{-5}$ dm$^3$ mol$^{-1}$ s$^{-1}$) are most appropriate, but it must be considered that variations in other parameters can significantly change the rate of reaction. Thus, the evidence based on the rate of reaction alone is insufficient to validate the conclusion that $k_a$ is negligible. However, this assumption is likely to be quite accurate, given the drastic reduction in rate in the presence of polybutadiene compared with bulk experiments.

The values of both $k_d$ and $k_{tr,P}$ used in the simulations are subject to considerable uncertainty. The effects of variation of these parameters was investigated by varying the input values of $k_{tr,P}$ by a factor of 2 in either direction and by decreasing $k_d$ by a factor of 2. The uncertainties in these parameters may be somewhat larger, but it can be observed from the results of these variations in Figures 11 and 12 that the effects of these uncertainties are quite significant, and more than account for any other uncertainties in input parameters, or discrepancies between predicted and observed rates of reaction. That is, the quantitative differences between simulation and experiment can easily be accounted for by the uncertainties in either of these parameters. Thus, the agreement between simulation and experiment is acceptable, but, because of the large effects of the uncertainties in the input parameters, this cannot be taken as proof that the model is correct. However, the shapes of the curves, and the relatively good agreement between simulation and experiment, show that the model is consistent with the experimental observations.

A problem with matching of the curves between simulation and experiment was that the predicted curvature of the rate curves was always greater than experimentally observed. This was especially apparent at 90 °C (Figure 4), where the simulated curves are distinctly curved, whereas the experimental curves were quite linear. Factors that were found to influence the

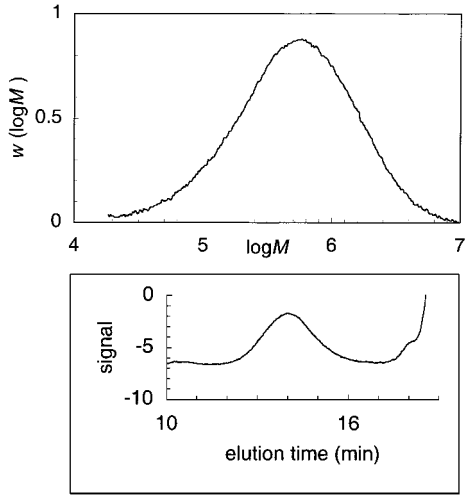


**Figure 13.** GPC distribution $w(\log M)$ (the GPC trace with baseline subtracted and corrections for nonlinear calibration) and the raw GPC trace for run 3.

**Table 2. Average Molecular Weights of Poly(VnD) Obtained from GPC**

| run | % conv | $\bar{M}_w/10^4$ | $\bar{M}_n/10^4$ | $\bar{M}_w/\bar{M}_n$ | $\bar{M}_n/10^4$ calcd from eq 9 |
|---|---|---|---|---|---|
| bulk | 14 | 40.0 | 10.5 | 3.8 | not applicable |
| 2 | 4 | 7.1 | 2.7 | 2.7 | 1.6 |
| 3 | 16 | 31.0 | 7.0 | 4.4 | 8.2 |
| 5 | 7 | 6.3 | 2.5 | 2.6 | 2.8 |
| 8 | 4 | 3.9 | 1.9 | 2.0 | 0.80 |
| 9 | 3 | 1.7 | 0.5 | 3.2 | 0.40 |

predicted curvature were the values of $k_d$ and $k_a$ (Figures 11 and 12). A decrease in $k_d$ not only decreases the rate of reaction but also results in a slower decrease in initiator concentration and, thus, a greater linearity of the rate of reaction. Increasing the value of $k_a$ not only increases the rate of reaction but also decreases the effects on the rate of reaction due by chain stoppage due to transfer to polymer. Other input parameters had minimal effect on the curvature. Reasonable variations in the input parameters could not account for the discrepancies in curvature at 90 °C, although the agreement could be improved. The reasons for this discrepancy are not known, but suggest that either (a) some of the assumptions of the model are inaccurate or (b) the values of some input parameters are incorrect by a significant margin (this seems unlikely, since the quantitative accord with the rate of reaction is acceptable, although also difficult to discount, since errors in $k_d$ may be significant, and also have an enormous effect on the calculation of $k_{tr,P}$, so that mutual cancellation of errors may result) or (c) there are further significant processes not accounted for in the basic model that become important at higher temperatures.

The results of these simulations show that the mathematical approximations used to deduce eq 7 are valid under most conditions. The simulations also provide an adequate fit to the experimental data, which of course is merely a consistency test given that the values of $k_{tr,P}$ used in the simulations were obtained from experiment using eq 7.

**GPC Analysis of PolyVnD.** The average molecular weights and molecular weight distributions of some samples of free polyVnD are shown in Table 2 and Figure 13. The branched or backbone polybutadiene eluted separately from the free polyVnD (see Figure 13), such that the free polyVnD could be treated as simple linear polyVnD for GPC analysis.

If the reaction follows the kinetics given above and the assumptions leading to eq 7 are valid, then the instantaneous molecular weight distribution should be a Flory−Schulz most probable distribution (exponential number molecular weight distribution), with a polydispersity of 2 and the number-average molecular weight $\bar{M}_n$ given by[25]

$$\bar{M}_n = M_0 \frac{k_p[M]}{k_{tr,P}[B]} \tag{9}$$

where $M_0$ is the molecular weight of the VnD monomer. Since the conversions examined here are relatively low, it is reasonable to take the monomer concentration as constant, in which case the instantaneous and cumulative molecular weight distributions are the same.

The results in Table 2 for the molecular weight distribution show that there is adequate accord between the values of $\bar{M}_n$ predicted by eq 9 and those observed experimentally. However, the polydispersities are not always the expected value of 2. The GPC results shown in Figure 13 are for the GPC distributions $w(\log M)$, i.e., after baseline subtraction and correction for nonlinear calibration.[26,27] These GPC distributions for the present system and the values of $\bar{M}_n$ and $\bar{M}_w$ are quite sensitive to baseline subtraction, and so the best that can be said for the comparison between expected and observed $\bar{M}_n$ values in Table 2 is that they do not contradict the quantitative mechanistic interpretation and they qualitatively support the supposition that the main chain-stopping event is transfer from polybutadiene by polyVnD radicals.

**Rate-Determining Step for Transfer to Polybutadiene.** Although the Arrhenius parameters for $k_{tr,P}$ are subject to high uncertainty, as shown in the 95% contour in Figure 7, nevertheless it is possible to make some deductions as to the nature of the process involved. The species resulting from the transfer of a hydrogen from butadiene to a polyVnD radical is presumably an allylic polybutadiene radical, for example formed from the loss of an H from the tertiary carbon in the 1,2-vinyl structure.

The transfer reaction considered here is an unusual one, in that it is between two polymer species. It is therefore possible that the process is diffusion-controlled, as both the chain end of a polyVnD radical and a polybutadiene chain will be relatively immobile, even in this rubbery system. We therefore consider both chemical control (i.e., the rate-determining step in the transfer process being the actual removal of a hydrogen atom) and diffusion control (i.e., the rate-determining step being the diffusion to close proximity of the radical end of the polyVnD chain and any part of a polybutadiene chain).

**Chemical Control.** Some frequency factors for transfer of a hydrogen atom between a polymeric radical and a small species are $10^{5.5}$ dm$^3$ mol$^{-1}$ s$^{-1}$ for transfer to monomer for acrylates and methacrylates,[28] and $10^{6.4}$ dm$^3$ mol$^{-1}$ s$^{-1}$ for vinyl acetate.[29] Elementary consideration of the transition states involved for transfer[30,31] suggests that similar frequency factors will hold for other macroradical/small-molecule vinylic systems, since these frequency factors are determined largely by the geometry of the species, which is dominated by the fact that a hydrogen is being transferred from a vinylic

radical with a side group attached. For the present system, one has both species being polymeric, rather than one being small and the other polymeric; steric considerations show that this can only result in a reduction in the frequency factor compared to an analogous small-molecule/polymer system. It is therefore reasonable to expect the frequency factor for the chemical-controlled step not to exceed ca. $10^6$ dm$^3$ mol$^{-1}$ s$^{-1}$. If the rate-determining step in the present polyVnD−radical/polybutadiene system is indeed chemical, then Figure 7 implies that the activation energy would have to be less than 25 kJ mol$^{-1}$. Although there are no data in the literature on reactions with moderate similarity to that studied here, an activation energy of 25 kJ mol$^{-1}$ is comparable to that of propagation and seems unlikely. However, chemical control cannot be unequivocally discounted, since the resulting species is allylic and a late transition state would therefore favor a relatively low activation energy.

**Diffusion Control.** The diffusion-controlled rate coefficient can be calculated by the model developed by Russell et al.[20−23] In brief, it is assumed that reaction always occurs when the reactive centers (in this case the end of a polyVnD radical and any monomer unit on polybutadiene) diffuse within a critical distance $\sigma$, which is taken as the Lennard-Jones radius of a monomer unit. The diffusion-controlled rate coefficient $k_{diff}$ is then given by

$$k_{diff} = 4\pi D\sigma N_A \tag{10}$$

where $D$ is the mutual diffusion coefficient of the reacting centers and $N_A$ is the Avogadro constant. The mutual diffusion coefficient is normally taken as the sum of those of each reacting center. Each of these diffusion coefficients in turn is the sum of a center-of-mass term $D_{cofm}$ and a reaction−diffusion term $D_{rd}$, the latter referring to the motion of a radical chain end by propagating. $D_{cofm}$ for a polymer of degree of polymerization $i$ was estimated from the "universal" empirical scaling law obtained by Griffiths et al.,[24] viz., $D_{cofm} = i^{-0.66-2.02w_p}D_{mon}$, where $D_{mon}$ is the monomer diffusion coefficient at the particular weight fraction of polymer $w_p$. $D_{rd}$ is given by $^1/_3\ k_p[M]a^2$, where, in a constrained system, $a$ is the root-mean-square end-to-end distance per square root of the number of monomer units in a polymer chain and can be approximated by $\sigma$. The value of $D_{mon}$ for a rubbery system such as the present, for a given $w_p$ and temperature, can be roughly estimated from the fits given by Griffiths et al.,[24] including an activation energy of 20 kJ mol$^{-1}$ for $D_{mon}$. It is this activation energy which is found to dictate the calculated value of the activation energy for $k_{diff}$. If it is assumed that all butadiene units in a polybutadiene chain are mobile, then this motion dominates the diffusion-controlled rate coefficient. The calculated activation energy is approximately that of $D_{mon}$, ≈ 20 kJ mol$^{-1}$, which is consistent with experiment; however, the calculated frequency factor is 5 orders of magnitude larger than that observed. If one assumes instead that it is the motion of the radical chain end of polyVnD that is rate-determining, then one obtains $k_{diff}$ (dm$^3$ mol$^{-1}$ s$^{-1}$) ≈ $10^8$ exp(−21 kJ mol$^{-1}$/$RT$), the frequency factor being slightly dependent on $w_p$. (It is interesting that the combination of the high value of $k_p$ for VnD, ≈ 5 × $10^3$ dm$^3$ mol$^{-1}$ s$^{-1}$ at 50 °C, and the relatively high monomer concentration, makes the reaction−diffusion term contribute significantly to the overall diffusion-controlled rate coefficient under these conditions, since the magnitude of the center-of-mass and reaction−diffusion terms are comparable). The activation energy is consistent with experiment, but the frequency factor is then about 2 orders of magnitude too high. It is not unreasonable to postulate that the hindrance involved in the reaction of the end of a macroradical with a site on another polymer chain could reduce the rate coefficient by such a factor, since the diffusion-controlled model assumes that the two species react as soon as they meet, no matter what their angle of encounter.

**Grafting Frequency of polyVnD to Polybutadiene.** There are only a few reliable data for the rate coefficient of transfer to polymer found in the literature due to the difficulties involved experimentally. The most used values, therefore, are from small model compounds analogous to that of the polymer. These values may not necessarily be accurate since these small radical−polymer reactions are in general "chemically controlled", and the polymeric radical−polymer reactions could indeed be "diffusion-controlled". The transfer coefficients obtained from this work should be taken as good approximate values, since they are consistent with GPC data and kinetic simulations. Thus, these values should also provide semiquantitative data for the grafting frequency of VnD to polybutadiene: that is, the number of polyVnD grafts per polybutadiene chain. Huang and Sundberg[12−15] give a complete kinetic description of all grafting reactions; the kinetic description given below is specific to retardative chain transfer with no reinitiation of the polybutadiene radicals.

The instantaneous grafting efficiency, $\phi$, is given by

$$\phi = \frac{\text{rate of change of mass of graft chains}}{\text{rate of change of mass of all chains}} \tag{11}$$

which can also be defined as the fraction of all polymerized monomer units that are grafted. In our case (retardative chain transfer), the rate of polyVnD radicals grafting to polybutadiene is simply the rate at which these radicals terminate with polybutadiene radicals, and the rate for all chains is equivalent to the rate of propagation. One then has the expression for the instantaneous grafting efficiency

$$\phi = \frac{k_{tr,P}[B]}{k_p[M]} \tag{12}$$

The instantaneous graft efficiency at low conversions is approximately equivalent to the time-average graft efficiency, $\Phi$ (so $\Phi = \phi$). Therefore, the graft frequency has the following relationship with respect to $\phi$:

$$\text{graft frequency} = \frac{[M(t=0)]x\phi\bar{M}_n^{PB}}{[PB]\bar{M}_n} \tag{13}$$

Here $x$ is the fraction conversion, $\bar{M}_n^{PB}$ is the number-average molecular weight of the polybutadiene, $\bar{M}_n$ is that of the polyVnD, and [PB] is the concentration of polybutadiene chains. The graft frequency calculated from eq 13 as a function of polybutadiene monomer unit concentration for conversions greater than 3% is shown in Figure 14. At the highest amounts of polybutadiene present in our system, a grafting frequency of ≈0.01 graft per polybutadiene chain is predicted. Temperature is predicted to have little effect on the graft frequency, due to the low activation energy determined for transfer.

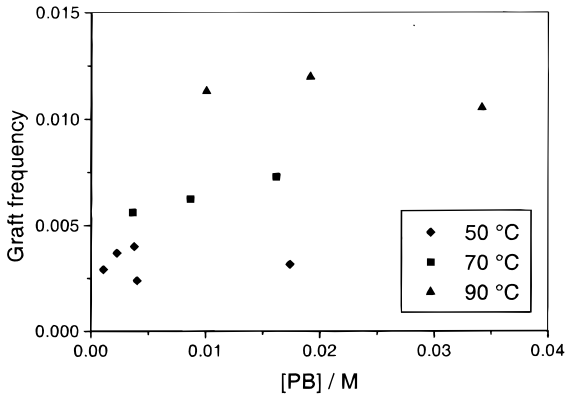


**Figure 14.** Predicted effect of [PB] on the graft frequency at 50, 70, and 90 °C for conversions greater than 3%; calculated from eq 13.

These results suggest that when the $\bar{M}_n$ of polybutadiene increases from the value of 5000 used in the present system to a value close to the much larger values in an emulsion system, the number of polyVnD grafts per polymer chain should increase drastically. At very high values of graft frequency, this will create a polymer microstructure consisting of small chain length polyVnD chains spread frequently across the polybutadiene chains. These grafting reactions can also form highly cross-linked networks.

## Conclusions

The retardative chain transfer mechanism is valid for vinyl neodecanoate (VnD) polymerization in polybutadiene, resulting in a highly grafted polymer microstructure. The rate coefficient for transfer to polymer was found to be $10^{6.9}$ dm$^3$ mol$^{-1}$ s$^{-1}$ exp(−27.6 kJ mol$^{-1}$), subject to high uncertainties. The results are consistent with the process being controlled either by the diffusion of the radical chain end, both by center-of-mass diffusion and "reaction−diffusion", or by the transfer step having a surprisingly low activation energy (this latter is considered less likely).

**Acknowledgment.** The support of the Australian Research Council and Elf-Atochem and helpful interactions with Drs Jean-Francis Pierson and Denis Tembou Nzudie of that company are gratefully acknowledged. The Key Centre for Polymer Colloids is established and supported under the Australian Research Council's Research Centres Program.

## References and Notes

(1) Lovell, P. A.; Shah, T. H.; Heatley, F. *Polym. Commun.* **1991**, *32*, 98.
(2) Lovell, P. A.; Shah, T. H.; Heatley, F. In *Polymer Latexes − Preparation, Characterization and Applications*; Daniels, E. S., Sudol, E. D., El-Aasser, M., Eds.; ACS Symposium Series 492; American Chemical Society: Washington, DC, 1992; p 188.
(3) Lovell, P. A. *Macromol. Symp.* **1995**, *92*, 71.
(4) Ahmad, N. M.; Heatley, F.; Lovell, P. A. *Macromolecules* **1998**, *31*, 2822.
(5) Britton, D.; Heatley, F.; Lovell, P. A. *Macromolecules* **1998**, *31*, 2828.
(6) Balic, R.; Gilbert, R. G.; Zammit, M. D.; Davis, T. P.; Miller, C. M. *Macromolecules* **1997**, *30*, 3775.
(7) Subramaniam, N.; Balic, R.; Taylor, J. R.; Griffiths, M.; Monteiro, M. J.; Gilbert, R. G.; Ho, C. C.; Abdullah, I.; Cacioli, P. *J. Nat. Rubber Res.* **1997**, *12*, 223.
(8) Subramaniam, N.; Monteiro, M. J.; Taylor, J. R.; Simpson-Gomes, A.; Gilbert, R. G. *Macromol. Symp.*, in press.
(9) Allen, P. W.; Merrette, F. M. *J. Polym. Sci.* **1956**, *22*, 193.
(10) Manaresi, P.; Passalacqua, V.; Pilati, F. *Polymer* **1975**, *16*, 520.
(11) Bevington, J. C. *J. Chem. Soc. London* **1954**, *4*, 3707.
(12) Huang, N. J.; Sundberg, D. C. *J. Polym. Sci.* **1995**, *33*, 2533.
(13) Huang, N. J.; Sundberg, D. C. *J. Polym. Sci.* **1995**, *33*, 2551.
(14) Huang, N. J.; Sundberg, D. C. *J. Polym. Sci.* **1995**, *33*, 2571.
(15) Huang, N. J.; Sundberg, D. C. *J. Polym. Sci.* **1995**, *33*, 2587.
(16) Santee, E. R.; Chang, R.; Morton, M. *J. Polym. Sci., Polym. Lett. Ed.* **1973**, *11*, 449.
(17) *Polymer Handbook*, 4th ed.; Brandrup, J., Immergut, E. H., Grulke, E. A., Eds.; John Wiley & Sons: New York, 1999.
(18) Moad, G.; Solomon, D. H. *The Chemistry of Free Radical Polymerization*; Pergamon: Oxford, England, 1995.
(19) van Herk, A. M. *J. Chem. Educ.* **1995**, *72*, 138.
(20) Scheren, P. A. G. M.; Russell, G. T.; Sangster, D. F.; Gilbert, R. G.; German, A. L. *Macromolecules* **1995**, *28*, 3637.
(21) Russell, G. T.; Napper, D. H.; Gilbert, R. G. *Macromolecules* **1988**, *21*, 2133.
(22) Russell, G. T.; Gilbert, R. G.; Napper, D. H. *Macromolecules* **1992**, *25*, 2459.
(23) Russell, G. T.; Gilbert, R. G.; Napper, D. H. *Macromolecules* **1993**, *26*, 3538.
(24) Griffiths, M. C.; Strauch, J.; Monteiro, M. J.; Gilbert, R. G. *Macromolecules* **1998**, *31*, 7835.
(25) Gilbert, R. G. *Emulsion Polymerization: A Mechanistic Approach*; Academic: London, 1995.
(26) Shortt, D. W. *J. Liq. Chromatogr.* **1993**, *16*, 3371.
(27) Clay, P. A.; Gilbert, R. G. *Macromolecules* **1995**, *28*, 552.
(28) Maeder, S.; Gilbert, R. G. *Macromolecules* **1998**, *31*, 4410.
(29) De Bruyn, H. Ph.D. Thesis, Sydney University,1998.
(30) Heuts, J. P. A.; Sudarko; Gilbert, R. G. *Macromol. Symp.* **1996**, *111*, 147.
(31) Huang, D. M.; Monteiro, M. J.; Gilbert, R. G. *Macromolecules* **1998**, *31*, 5175.

MA990604R